ACS APPLIED MATERIALS & INTERFACES

Research Article

www.acsami.org

Thermal Evaporation versus Spin-Coating: Electrical Performance in Columnar Liquid Crystal OLEDs

Juliana Eccher,*[,†,‡] Wojciech Zajaczkowski,[∥] Gregório C. Faria,[§] Harald Bock,[⊥] Heinz von Seggern,[‡] Wojciech Pisula,[∥,#] and Ivan H. Bechtold*[,†]

[†]Departamento de Física, Universidade Federal de Santa Catarina—UFSC, 88040-900 Florianópolis, Santa Catarina, Brazil

[‡]Department of Electronic Materials, Institute of Materials Science, Technical University of Darmstadt, Petersenstrasse 23, D-64287 Darmstadt, Germany

[∥]Max Planck Institute for Polymer Research, Ackermannweg 10, 55128 Mainz, Germany

[§]Instituto de Física de São Carlos, Universidade de São Paulo, PoB.:369, 13560-970 São Carlos/SP, Brazil

[⊥]Centre de Recherche Paul Pascal, Université de Bordeaux & CNRS, 115 Avenue Schweitzer, 33600 Pessac, France

[#]Department of Molecular Physics, Faculty of Chemistry, Lodz University of Technology, Zeromskiego 116, 90-924 Lodz, Poland

Supporting Information

ABSTRACT: The electrical responses of a columnar liquid crystal (a diimidodiester derivative of benzo[*ghi*]perylene) deposited either by spin-coating or by thermal evaporation into a typical OLED device are compared. For the spin-coated film, homeotropic alignment was induced by thermal annealing, which enhanced the charge carrier mobility significantly. For the evaporated films, homeotropic alignment could not be obtained by annealing. However, a degree of rectification higher than 3 orders of magnitude was achieved, even without annealing, with an electrical response similar to the response of the aligned spin-coated film. A trap-limited space−charge-limited current model was used to extract the charge carrier mobility directly from the current−voltage curves. Grazing incidence wide-angle X-ray scattering confirmed the homeotropic alignment of the annealed spin-coated film, whereas the columns are mostly oriented parallel to the surface in the evaporated case. In a field-effect transistor with bottom-gate bottom-contact geometry, the evaporated film exhibited a typical behavior of an n-type transistor. The degree of intermolecular order is thereby strongly dependent on the deposition method where vacuum deposition leads to a higher order. This higher order, however, impedes reorientation by annealing of the evaporated film but leads to improved charge transport between the electrodes even without homeotropic alignment of columnar liquid crystal.

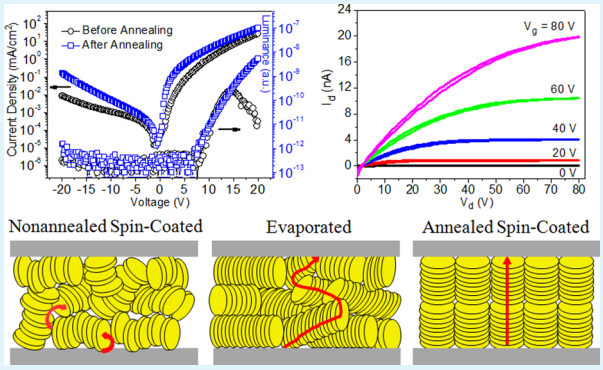

KEYWORDS: *columnar liquid crystals, optoelectronic devices, molecular packing, processing, current rectification*

1. INTRODUCTION

Liquid crystals (LCs) are a fascinating class of soft materials due to their combined properties of fluidity and long-range order. Recently, these materials have been recognized for various optoelectronic applications, and new research lines are being investigated.[1−3] Columnar liquid crystals (ColLCs) are emerging as one-dimensional organic charge transport materials, providing good charge carrier mobility along the columns.[4−6] In the columnar phase π-stacking between aromatic cores can provide a facile path for charge transport via hopping from one molecule to another.[7] Thus, LCs have attracted special attention from the scientific community as promising self-organized molecular semiconductors due to their potential application in organic electronics,[8,9] including organic field effect transistors (OFETs),[10] organic solar cells (OSCs),[11] and organic light emitting diodes (OLEDs).[12] LCs can be easily processed since they can be spin-coated in the form of thin films from solution like polymers or by vacuum deposition like most small molecules. One important characteristic of these materials is the property of self-healing, i.e., the ability of the mesophase to repair spontaneously structural defects, which are likely to act as traps for charge carriers.[13−15]

In ColLCs the local molecular orientation and the intermolecular distance of neighboring aromatic cores within the columns exert a strong influence on the charge transport.[16,17] High charge carrier mobilities, up to 1.1 $cm^2/(V\,s)$ for p-type liquid crystalline semiconductors[18,19] and up to 6 $cm^2/(V\,s)$ for n-type liquid crystalline semiconductors,[20] have been

Received: April 23, 2015
Accepted: July 13, 2015
Published: July 13, 2015

DOI: 10.1021/acsami.5b03496
ACS Appl. Mater. Interfaces 2015, 7, 16374−16381

found. Hole transport is observed in a great variety of organic materials, whereas electron transport is limited to a few classes of materials.[16] ColLCs based on the perylenediimide core have been successfully used as electron acceptor materials in OSCs, OFETs, and OLEDs,[21] exhibiting charge mobilities of up to 1.3 $cm^2/(V\ s)$.[22]

In the present article it is described how the deposition method (spin-coating versus thermal evaporation) influences the molecular packing and the intermolecular order of a diimidodiester derivative of benzo[*ghi*]perylene. It was observed that the higher molecular order, induced by vacuum deposition, improved the charge transport along the columns. As determined by GIWAXS measurements, even that in the evaporated films the columns are mostly oriented parallel to the surface, a rectification rate of 3 orders of magnitude in a diode configuration was obtained. The current−voltage curves were fitted with a trap-limited space−charge-limited current model to extract the carrier mobility of the material. In a bottom-gate bottom-contact transistor structure, the evaporated films revealed an n-type behavior.

2. EXPERIMENTAL SECTION

The synthesis of the columnar liquid crystal (ColLC) used here, benzo[*ghi*]perylene-1,2,4,5,10,11-hexacarboxylic-1,2-bis(2-ethylhexyl)-ester-4,5:10,11-bis(undec-4-yl)imide, has been published elsewhere[23] as well as its characterization as spin-coated active layer in diode structures.[24] The chemical structure is shown in Figure 1.

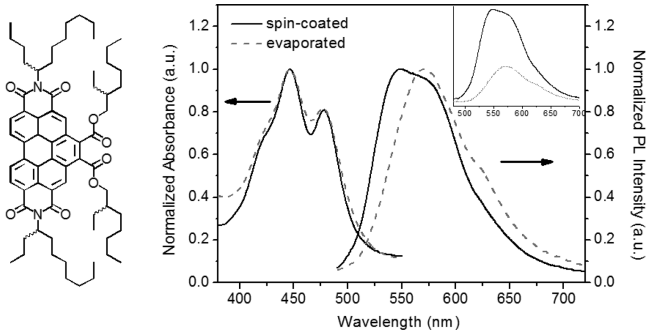

Figure 1. Molecular structure, absorption, and fluorescence spectra of the spin-coated (solid) and evaporated (dashed) films of the ColLC. Inset: non-normalized photoluminescence spectra.

The absorption and fluorescence spectra for the solid state were collected with an OceanOptics USB4000 spectrophotometer. Measurements were performed on evaporated films on glass substrates.

Atomic force microscopy (AFM) was applied to inspect the morphology of the evaporated films, using an Asylum Research MFP-3D in tapping mode with a scanning rate of 0.10 Hz covering a size of 10 μm × 10 μm with 512 × 512 lines.

GIWAXS was performed to gain structural information on the spin-coated and evaporated films. The measurements were done by means of a solid anode X-ray tube (Siemens Kristalloflex X-ray source, copper anode X-ray tube (λ = 1.5418 Å) operated at 30 kV and 20 mA), osmic confocal MaxFlux optics, X-ray beam with pinhole collimation, and a MAR345 image plate detector. GIWAXS measurements of the films deposited by thermal evaporation after thermal annealing were performed at the DELTA Synchrotron using beamline BL09 with a photon energy of 10 keV (λ = 1.2398 Å). The beam size was 0.05 mm × 0.5 mm, and samples were irradiated just below the critical angle for total reflection with respect to the incoming X-ray beam (~0.18°). The scattering intensity was detected on a 2-D image plate (MAR-345) with a pixel size of 150 μm (2300 × 2300 pixels), and the detector was placed 345 mm from the sample center. Data analysis was performed using the Datasqueeze software.

For the electrical characterization, indium tin oxide (ITO) coated glass plates with a sheet resistance of about 15 Ω/o were used as conductive substrates. After proper substrate cleaning, a thin layer of poly(3,4-ethylenedioxythiophene):poly(styrenesulfonate) (PEDOT:PSS) was deposited by spin-coating at 3000 rpm during 30 s, followed by annealing at 110 °C for 5 min. The organic layer was deposited by spin-coating at 2000 rpm for 30 s using a 50 mg/mL *n*-heptane solution and by thermal evaporation in high vacuum (10^{-7} mbar) at a deposition rate of 2 Å/s. The thickness of the evaporated film was probed with a Dektak 8000 profilometer. Top electrodes were obtained by a successive vacuum deposition (10^{-7} mbar) of Ca (50 nm) and Al (100 nm) at a deposition rate of 2 Å/s. The active area of the diode was 10 mm^2. Devices were annealed on a hot plate at 120 °C for 4 h in order to achieve homeotropic alignment, followed by cooling to room temperature. The *J*/*V* curves were measured at room temperature (25 °C) using a HP Semiconductor Parameter Analyzer (Model 4145A).

The bottom-gate, bottom-contact OFET substrates were purchased from the Fraunhofer Institute for Photonic Microsystems in Dresden, Germany. Highly n-doped silicon with a thin layer (~230 nm and capacitance of 1.5 × 10^{-4} F/m^2) of silicon dioxide acts as the gate electrode and insulator, respectively. The source-drain (30 nm Au with a 10 nm ITO high work function adhesion layer) electrodes possess an interdigital structure with a channel length of 20 μm and a channel width of 10 mm. The organic layer was deposited on the cleaned device substrate by thermal evaporation in high vacuum (10^{-7} mbar) at a deposition rate of 2 Å/s. The transistors were characterized at room temperature (25 °C) using a HP Semiconductor Parameter Analyzer (Model 4155A).

3. RESULTS AND DISCUSSION

Photophysical Properties. The absorption and fluorescence spectra of the spin-coated and evaporated ColLC films showed the same vibronic structure with two main peaks at 445 and 477 nm (Figure 1). This indicates that the molecular structure is preserved after the sublimation process. The photoluminescence maximum of the evaporated film coincides with the shoulder of the spin-coated one at 575 nm. This shoulder vanishes above the columnar to isotropic phase transition and can be related to the π-stacking aggregation.[24] This fact suggests that the π-stacking aggregates are stronger in the evaporated film. Furthermore, the emission of the evaporated film is less intense than that of the spin-coated film (films of same thickness) (inset in Figure 1). This photoluminescence suppression also supports the enhanced molecular packing expected in the evaporated film.

Grazing Incidence Wide-Angle X-ray Scattering. When the ColLC was deposited by spin-coating followed by deposition of the metallic electrodes in a typical diode structure (ITO/PEDOT:PSS/ColLC/Ca/Al) and annealed at 120 °C for 3 h, homeotropic alignment was obtained only under the metallic layer.[24] Therefore, the presence of the second electrode surface (Ca/Al) plays an important role for alignment of spin-coated films. Homeotropic alignment by thermal annealing of a columnar liquid crystal spin-coated between a glass plate and a metallic electrode has been achieved previously in Brunet et al.,[25] where the confining effects due to the silver electrode were verified. Accordingly, we investigated by GIWAXS the alignment of evaporated films under an upper metal electrode and without the covering electrode.

GIWAXS measurements performed in the open area of the spin-coated film after annealing of the device at 120 °C for 3 h show a typical pattern of a hexagonal unit cell with edge-on arranged molecules (a_{hex} = 2.21 nm; π-stacking distance = 0.37

DOI: 10.1021/acsami.5b03496
ACS Appl. Mater. Interfaces 2015, 7, 16374−16381

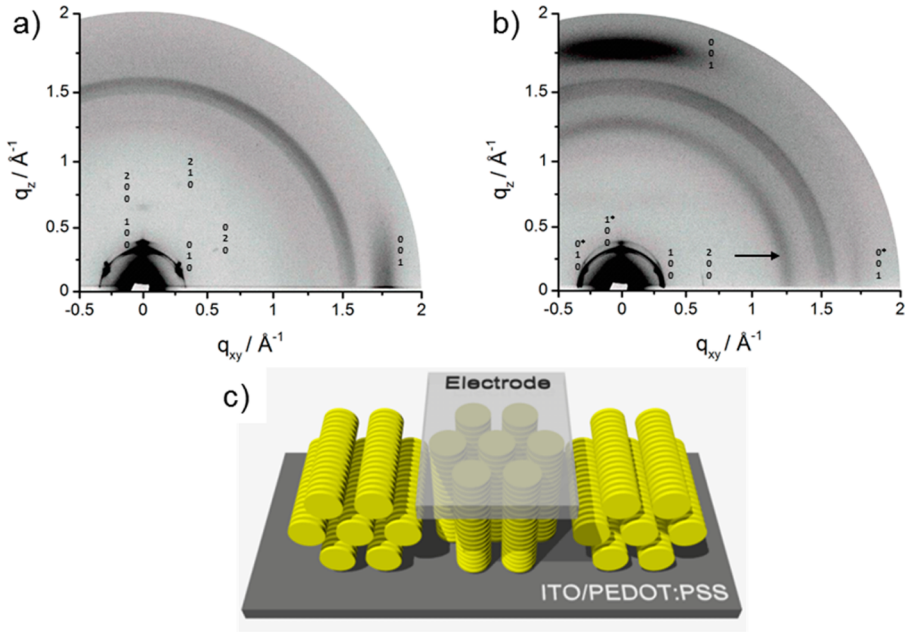

Figure 2. GIWAXS patterns of annealed spin-coated ColLC film measured (a) in the open area and (b) in the electrode area (the arrow points toward the isotropic reflection related to the metal electrode, reflections are assigned by Miller's indices, reflections* are attributed to the minor edge-on fraction), (c) schematic illustration of the molecular organization in the open film (edge-on orientation) and in the region under the electrode (face-on orientation).

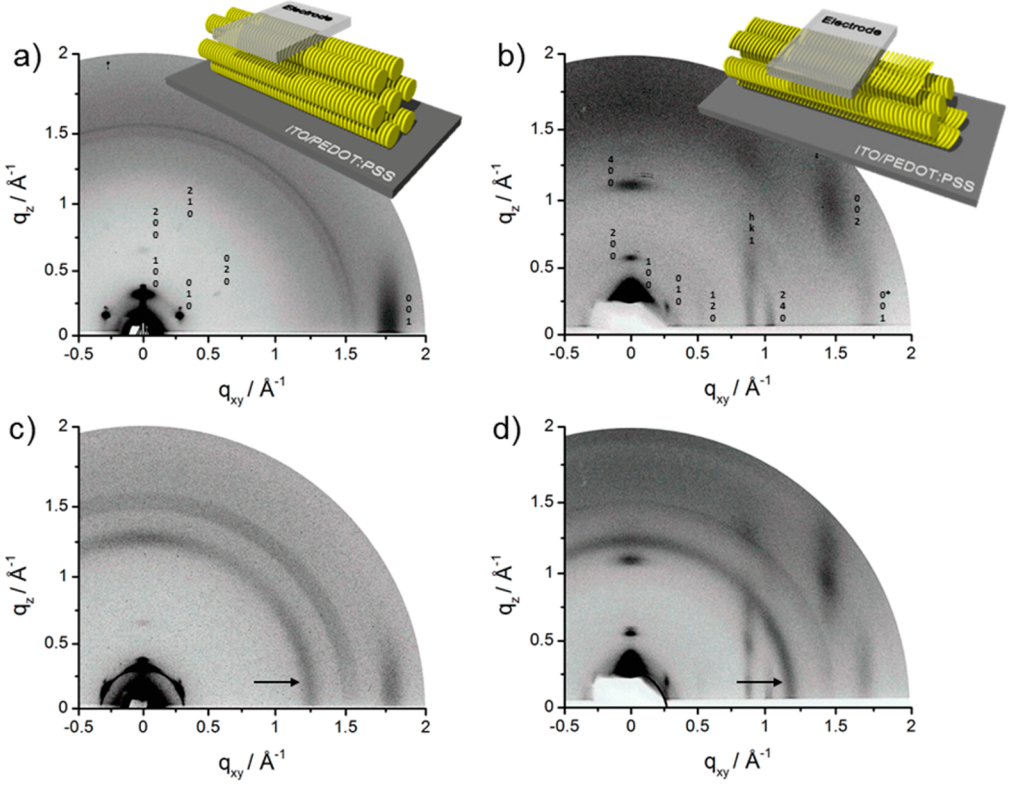

Figure 3. GIWAXS of evaporated ColLC film measured in the open area (a) before and (b) after annealing. Reflections are assigned by Miller's indices; reflections* are attributed to the minor edge-on fraction. GIWAXS of evaporated film under the electrode area (c) before and (d) after annealing (arrow indicates isotropic reflection of the metal electrode). Insets illustrate the corresponding molecular organization in the evaporated film before and after annealing.

nm). The scattering intensities are assigned by using Miller's indices in Figure 2a. The *h*00 and 0*k*0 peaks are related to the hexagonal intercolumnar arrangement, whereas the 001 reflection is attributed to in-plane π-stacking. Most probably several domains, which are randomly in-plane oriented, contribute to the scattering pattern leading to the appearance of π-stacking and intercolumnar reflections. In the area under the electrode, the initial edge-on arrangement turns into a

DOI: 10.1021/acsami.5b03496
ACS Appl. Mater. Interfaces 2015, 7, 16374−16381

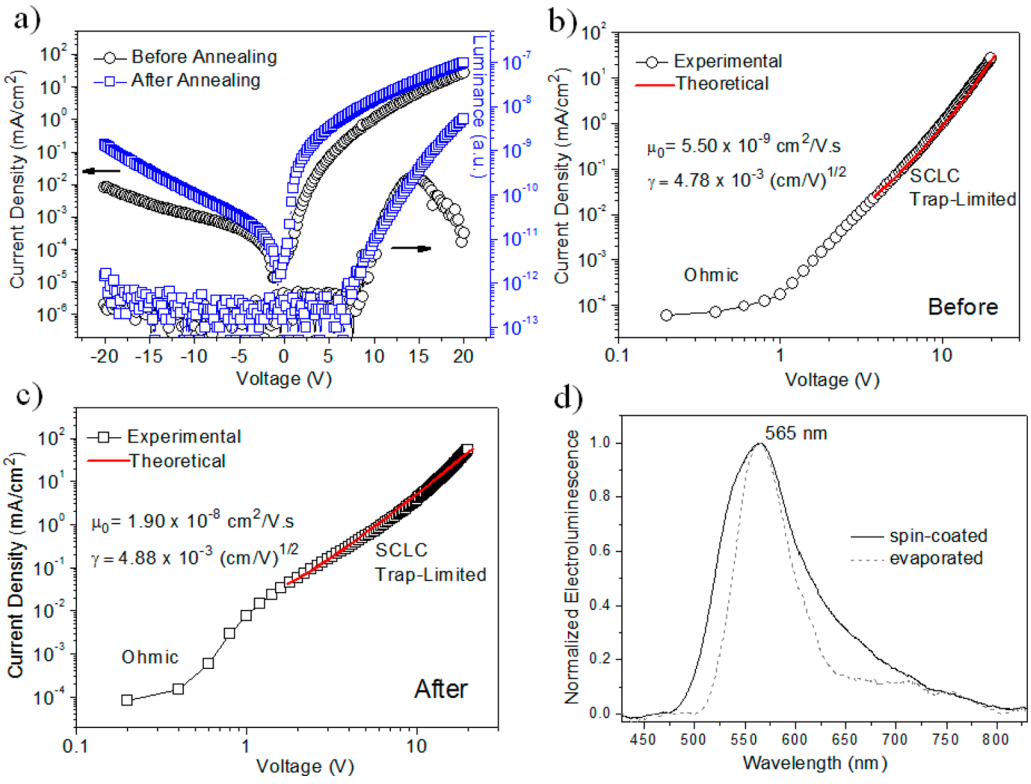

Figure 4. Electrical characterization of an evaporated film in a diode structure. (a) Current density (left) and luminance (right) versus voltage. (b) and (c) Log–log plots of the *J*–*V* curves for the device before and after annealing (120 °C for 4 h), respectively. The red solid lines indicate the fitting by trap-limited SCLC transport. (d) Electroluminescence spectra of devices for the spin-coated (solid) and evaporated (dashed) films obtained at 15 V. Black circles and blue squares represent the device before and after annealing, respectively.

major face-on orientation due to surface interactions (Figure 2b). This orientational transition is evident from the shift of the π-stacking 001 reflection (Figure 2a,b) from in-plane to out-of-plane. Interestingly, the π-stacking scattering intensity becomes more distinct in the face-on organization indicating higher intracolumnar order in this type of alignment. However, a minor edge-on fraction is still present in the electrode area as indicated by the weak reflections* related to in-plane π-stacking and the hexagonal unit cell. The GIWAXS measurements of the spin-coated films confirmed that the homeotropic alignment occurs only in the region under the metallic contact agreeing with the optical observations.[24]

To investigate the molecular organization and the thermal annealing effects for the evaporated films, GIWAXS measurements (Figure 3) were also performed for the diode structure in the regions outside and under the metallic electrode before and after annealing the device at 120 °C for 4 h. For the as-evaporated films three distinct scattering spots in the small-angle region can be observed which are characteristic for a hexagonal arrangement of columns. The hexagonal lattice parameter[26,27] determined from the *h*00 and 0*k*0 peak positions is a_{hex} = 2.15 nm and is in agreement with the value found for the bulk structure (Figure 3a). Thereby, the columnar axis is oriented parallel to the surface (inset in Figure 3a). The edge-on arrangement of the molecules was confirmed by in-plane π-stacking 001 reflection related to an intermolecular distance of 0.35 nm (Figure 3a). The unit cell parameters are identical to the bulk and verify liquid crystallinity also in the evaporated film.[23] After annealing the film at 120 °C for 4 h, significant changes in the structure of the film became evident by the appearance of new scattering peaks (Figure 3b). The increased number of reflections is characteristic for an increased crystallinity due to the thermal annealing. The π-stacking peak, labeled as 002, is shifted from in-plane to an off-equatorial position indicating a molecular tilting (inset in Figure 3b). Thereby, the molecular plane was tilted by ca. 30° toward the surface maintaining an unchanged intermolecular distance of 0.35 nm. However, a minor fraction of molecules remained edge-on as evident from the low intensity 001* reflection. The columnar arrangement is slightly distorted from the hexagonal lattice to an oblique one with parameters of a = 2.19 nm and b = 2.07 nm. Within the stacks the molecules are assembled in a staggered fashion as implied by an additional off-equatorial reflection at q = 0.92 Å^{-1} on the *hk1* scattering line related to the doubled π-stacking distance of 0.68 nm. In this packing motif neighboring molecules are flipped by 180° so that every second disc possesses an identical positional arrangement in the column.[28] The GIWAXS patterns in Figures 3c and 3d indicated that the molecular organization is not influenced by the presence of the metallic electrode as a second surface on top of the film. In contrast to the spin-coated films, the GIWAXS patterns for the evaporated films after annealing were almost identical in the open area and in the area under the electrode (compare Figures 3b and 3d). For the evaporated films, the increase in crystallinity and considerable reorganization are mainly attributed to the substrate. The importance of the surface on the initiation of nucleation and crystallinity has been reported for various polymers and also for discotic liquid crystals.[29,30]

In contrast to spin-coated films, homeotropic alignment was not induced in the area under the electrode for the evaporated film after thermal annealing at 120 °C for 4 h. This behavior

DOI: 10.1021/acsami.5b03496
ACS Appl. Mater. Interfaces 2015, 7, 16374–16381

can be attributed to the tight packing of molecular cores and side chains depending on the film processing method. According to the GIWAXS data, the intermolecular distances were larger in the spin-coated film than in the evaporated one indicating that the molecular packing is denser in the latter case. Even thermal annealing at higher temperatures for longer times (for example, at 130 °C for 6 h) does not lead to homeotropic alignment in the evaporated film. The alignment of ColLCs dependent on the deposition method has been studied previously in open films (without the electrode) by grazing incidence X-ray diffraction. In that work, homeotropic alignment was observed for spin-coated and evaporated films of a columnar pyrene derivative after thermal annealing.[31] An evaporated film of a columnar perylene derivative was also homeotropically oriented by thermal annealing and applied in Schottky-type devices.[32]

Electrical Characterization in a Diode Structure. The device structure used for electrical characterization of the evaporated films was ITO/PEDOT:PSS (45 nm)/ColLC (160 nm)/Ca (50 nm)/Al (100 nm). The thicknesses of the PEDOT:PSS (45 nm) and ColLC (160 nm) films were determined by a Dektak profilometer.

AFM measurements were performed to investigate the morphological aspects of the evaporated films. From those measurements, the mean-surface roughness (RMS) of the film was found to be 2.1 nm for an image of 10 μm × 10 μm (see the Supporting Information for details). This roughness is slightly smaller than the roughness obtained from spin-coated films, and both films exhibit quite similar morphology.

The electrical measurements were performed at room temperature in a controlled N_2 atmosphere before and after the annealing process (120 °C for 4 h). Figure 4a shows the current−density/voltage (J−V) and luminance/voltage (L−V) characteristics before (black circles) and after (blue squares) annealing at 120 °C. A degree of rectification higher than 3 orders of magnitude at 20 V was obtained before annealing. This result for the evaporated film is very interesting since for the spin-coated film only a low degree of rectification was observed before annealing. This suggests that in the evaporated film a superior molecular order exists prior to annealing. As the columnar domains are mostly oriented edge-on on the surface the better electrical response in a diode configuration supports a particularly dense molecular packing for the evaporated film, in which the close proximity of the molecules leads to improved charge migration through a strong π-orbital overlap. It can also be concluded that for the film produced by thermal evaporation the interfacial contact between the ColLC and the electrodes was improved. This is especially the case at the interface ColLC/PEDOT:PSS at the anode side leading to improved hole injection.

It can be seen that the turn-on voltage for the electroluminescence is higher than the threshold voltage for which the SCLC process becomes dominant, as was the case of the spin-coated film.[24] For the same electric field, the electroluminescence intensity for the evaporated film is 2 orders of magnitude higher than for the spin-coated film before annealing, indicating superior transport and injection processes in the evaporated film compared to the spin-coated film before annealing. A reduction of the electroluminescence intensity is observed above 15 V. This reduction is not related to a degradation of the organic material as can be seen from the renewed increase of the luminance upon reduction of the voltage. This reduction of the electroluminescence may be related to the quenching of excitons at the anode. As described previously the electron mobility of this material is higher than that of holes, and electron injection is easier than hole injection in this device configuration.[24] Consequently, the recombination of charge carriers occurs close to the anode. As the applied voltage increases above 15 V, the electrons seem to overwhelm the injected holes thereby reducing the radiative decay rate.

Upon annealing, the current density at 20 V increases by a factor of 2 (Figure 4a). A more pronounced increase in current density upon annealing can be observed at lower voltages (from 1 to 5 V) (Figure 4c). Thermal annealing is known to heal structural defects.[33] In the present case, it is possible that the thermal annealing reduces the number of trapping states or the average trap depth associated with structural defects (such as grain boundaries), and thus more charge carriers contribute to the current. After annealing, the electroluminescence does not decrease above 15 V anymore which can be related to an improvement in injection of holes and an increase hole mobility, favoring charge carrier recombination in a region more distant from the anode. It is also observed that the onset of electroluminescence (Figure 4a) was reduced from 8.4 to 6.8 V after annealing.

The log−log plots of the current densities for the evaporated film before and after annealing are displayed in Figures 4b and 4c, respectively. The conduction regimes follow an Ohmic behavior at low voltages and a trap-limited SCLC at higher voltages. The charge carrier mobility was obtained by fitting SCLC curves with an electric field dependent mobility, $\mu = \mu_0(T)e^{\gamma\sqrt{E}}$, to the experimental current−voltage characteristics. The underlying theoretical model was presented previously.[24] Thereby, values for μ_0 and γ were extracted before and after annealing, and corresponding current fits are displayed as red lines in Figures 4b and 4c. The fits for the trap-limited SCLC regime show very good agreement with experimental data with fitting parameters listed in Table 1. The Poole−Frenkel coefficient γ is higher after annealing, revealing that the hopping transport is easier for the annealed sample than for the nonannealed one. In Table 1 the values of mobility calculated from $\mu = \mu_0(T)e^{\gamma\sqrt{E}}$ are presented before and after annealing for an applied voltage of +20 V (see also the graphs of $\mu(V)$ in the Supporting Information).

Table 1. Fitting Values Obtained for μ_0 and γ

parameter	before annealing	after annealing
μ_0 (10^{-9} cm^2/(V s))	(5.50 ± 0.03)	(19.00 ± 0.03)
γ (10^{-3} cm/V)$^{1/2}$	(4.78 ± 0.02)	(4.88 ± 0.02)
μ at applied +20 V (10^{-6} cm^2/(V s))	(2.1 ± 0.1)	(6.5 ± 0.1)

μ_0 is the mobility at zero field, and γ resembles the Poole−Frenkel coefficient.

It was found that annealing leads to a threefold increase in charge carrier mobility in the trap-limited SCLC regime. This increase in mobility goes along with the increase in current density. Figure 4d shows the electroluminescence spectra for the devices with films produced by spin-coating (solid line) and by thermal evaporation (dashed line). The maximum intensity for both cases coincides at 565 nm, but the emission for the evaporated film is narrower, indicating a more ordered molecular organization. For the same diode structure, the ColLC material deposited by thermal evaporation presents intermediate electrical characteristics to those obtained by spin-coating without and with annealing. The electrical properties of

DOI: 10.1021/acsami.5b03496
ACS Appl. Mater. Interfaces 2015, 7, 16374−16381

the evaporated film were superior to the spin-coated film before annealing, but inferior to the electrical properties of the annealed spin-coated film. Figure 5 sketches the molecular packing and the charge transport for each case.

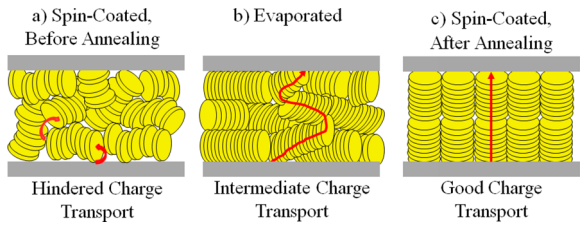

Figure 5. Molecular packing in the spin-coated films (a) before and (c) after annealing and in the (b) nonannealed evaporated film.

In the evaporated film the molecular packing is more ordered and denser than in the nonannealed spin-coated film, and, thus, the charge transport prior to annealing was higher in the evaporated film. On the other hand, in the spin-coated film after annealing, the face-on orientation provides an optimal condition for the charge transport in a diode device. The γ values indicate that transport via hopping in the aligned spin-coated film is more efficient than in the evaporated film.[24]

Electrical Characterization in a Transistor Structure. According to the GIWAXS measurements, the columnar domains in the evaporated film are preferably edge-on oriented on the surface. Therefore, the ColLC was deposited by thermal evaporation in a transistor structure in order to determine the in-plane mobility. The electrode geometry of the transistor possessed a channel length L = 20 μm and width W = 10 mm. The organic material was deposited on the device substrate at a thickness of 60 nm. Figure 6 shows the typical output and transfer characteristics of the transistor after annealing at 120 °C for 4 h. Although the source-drain currents (I_d) were very low of the order of 10^{-9} A, the device exhibited a clear n-type operation, where a current of electrons was measured between the source and drain electrodes for an applied positive voltage at the gate.

The reason for the low current value can be explained by the large energetic barrier (1.6 eV) for the electron injection from the gold electrode (5.2 eV) to the LUMO (3.6 eV) of the organic material. A comparison of Figure 6 and Figure S3 of the Supporting Information shows that after annealing for 4 h at 120 °C the current increases by a factor of 3 indicating an enhanced structural order. The respective mobility values of 3.8 × 10^{-7} and 1.3 × 10^{-6} $cm^2/(V\ s)$ before and after annealing were determined from the saturation regime,[34,35] plotting $(I_d)^{1/2}$ versus V_g for V_d = 80 V. The magnitude of the mobility obtained from the diode structure also increases by a factor of 3 in the case of the evaporated film after annealing and therefore is comparable to the increase observed for the OFET structure. The general behavior of an increased order in the diode structure is supported by the GIWAXS and $J-V$ measurements.

In contrast, when the ColLC material was deposited by spin-coating in the transistor structure (annealed or not annealed), the electrical characterization did not reveal an operating transistor. This fact also corroborates to the GIWAXS results which indicate beyond a preferred edge-on orientation, a denser molecular packing in the evaporated films.

4. CONCLUSION

It was shown that an electron-deficient columnar liquid crystalline benzo-perylene-diimidodiester can be deposited either by spin-coating or by thermal evaporation. The so-obtained films show molecular packing, annealing behavior, and electrical properties that depend strikingly on the film depositing method. The fluorescence spectrum of the evaporated film is red-shifted and less intense than the spin-coated film, indicating stronger π-stacking interactions. The functionality of the ColLC material was proven in a typical diode structure. The devices were thermally annealed at 120 °C for several hours in order to obtain a face-on orientation. GIWAXS measurements clearly prove in the case of the spin-coated film a homeotropic alignment under the metallic electrode. However, after applying the same thermal annealing to the evaporated film, the columnar domains remain edge-on oriented and no homeotropic alignment is observed in the region under the metallic electrode. Nevertheless, a pronounced rectification was obtained for the evaporated film even before annealing, showing a typical diode behavior. In contrast, for the spin-coated film this behavior was only obtained after the induction of homeotropic alignment by annealing. It is assumed that the denser molecular packing in the evaporated film does not allow a reorientation from edge-on to face-on by thermal annealing. On the other hand, this very dense molecular packing ensures an improved π-overlap between molecules to yield an efficient charge transport between the electrodes.

The $J-V$ characteristics revealed an initial Ohmic behavior at low voltages followed by a trap-limited SCLC regime at higher voltages. The SCLC transport can be described by a theoretical model[24] with an electric field dependent charge carrier mobility. The nonannealed organic film applied in the same diode structure showed much better rectification and emission for the evaporated sample in comparison to the spin-coated one. The

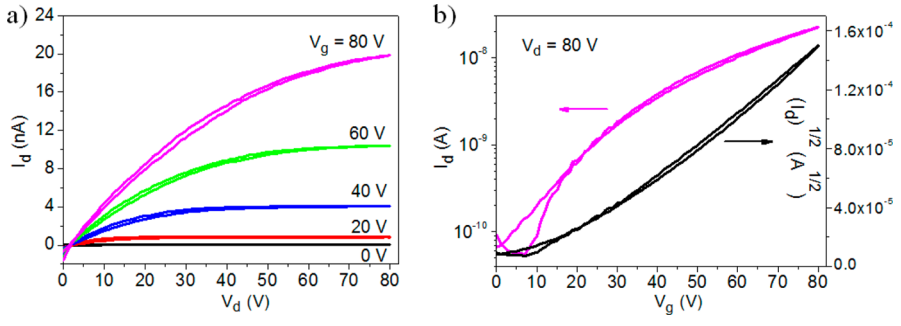

Figure 6. (a) Output characteristics and (b) transfer curves of the n-type transistor for the evaporated film after annealing at 120 °C for 4 h.

DOI: 10.1021/acsami.5b03496
ACS Appl. Mater. Interfaces 2015, 7, 16374−16381

evaporated film also exhibited typical n-type transistor behavior. Transistors with a spin-coated film did not present an expected characteristic behavior. The mobility values for the evaporated film were determined directly from the $J-V$ curves and from the transistor structure. Finally, this work provides valuable insights how the deposition method influences the electrical properties of a columnar liquid crystal in diodes and transistors. In addition, the thermal evaporation impeded the possibility of homeotropic alignment. Thereby, the best performance in an OLED device was obtained for the aligned spin-coated film. Despite this fact, comparing the spin-coated and evaporated films nonannealed in an OLED device, the evaporated one showed a higher current rectification and more intense luminance. In transistor devices only the evaporated film revealed a clear operating transistor. In summary, due to the superior molecular packing in the evaporated films they can be applied either in diode or transistor, showing a satisfactory electrical response.

■ ASSOCIATED CONTENT

Supporting Information

AFM analysis of the evaporated film, charge carrier mobilities in the SCLC regime as a function of the voltage for the device before and after annealing, and output and transfer characteristics of transistor before annealing. The Supporting Information is available free of charge on the ACS Publications website at DOI: 10.1021/acsami.5b03496.

■ AUTHOR INFORMATION

Corresponding Authors

*Phone: +55 48 37212304. Fax: +55 48 37219946. E-mail: juh_19@yahoo.com.br.

*Phone: +55 48 37212304. Fax: +55 48 37219946. E-mail: ivan.bechtold@ufsc.br.

Notes

The authors declare no competing financial interest.

■ ACKNOWLEDGMENTS

The authors thank the following institutions for financial support: CAPES, COFECUB (project PL-C 803-14) CNPq, and INCT/INEO. G.C.F. acknowledges the fellowship by the "Fundação de Amparo à Pesquisa do Estado de São Paulo" (FAPESP) (Proc-number 2013/21034-0. H.v.S. acknowledges the scholarship "Special Visiting Researcher" by the Brazilian Science without Borders Program (CNPq and Capes−Proc-number 400133/2012-1). The authors gratefully acknowledge the beamline 9 of the DELTA electron storage ring in Dortmund for providing synchrotron radiation and technical support for GIWAXS measurements.

■ REFERENCES

(1) Lagerwall, J. P. F.; Scalia, G. A New Era for Liquid Crystal Research: Applications of Liquid Crystals in Soft Matter Nano-, Bio- and Microtechnology. *Curr. Appl. Phys.* **2012**, *12*, 1387−1412.

(2) Acharya, B. R.; Choi, H.; Srinivasarao, M.; Kumar, S. Homeotropically Aligning Phase Separated Columnar Structures for Fabrication of Flexible Electrooptical Devices. *Appl. Phys. Lett.* **2011**, *99*.22110810.1063/1.3663966.

(3) Toth, K.; Molloy, J. K.; Matta, M.; Heinrich, B.; Guillon, D.; Bergamini, G.; Zerbetto, F.; Donnio, B.; Ceroni, P.; Felder-Flesch, D. A Strongly Emitting Liquid-Crystalline Derivative of Y3N@C-80: Bright and Long-Lived Near-IR Luminescence from a Charge Transfer State. *Angew. Chem., Int. Ed.* **2013**, *52*, 12303−12307.

(4) Kaafarani, B. R. Discotic Liquid Crystals for Opto-Electronic Applications. *Chem. Mater.* **2011**, *23*, 378−396.

(5) Bushby, R. J.; Kawata, K. Liquid Crystals That Affected the World: Discotic Liquid Crystals. *Liq. Cryst.* **2011**, *38*, 1415−1426.

(6) O'Neill, M.; Kelly, S. M. Ordered Materials for Organic Electronics and Photonics. *Adv. Mater.* **2011**, *23*, 566−584.

(7) Kumar, S. Discotic Liquid Crystal−Nanoparticle Hybrid Systems. *NPG Asia Mater.* **2014**, *6*.e8210.1038/am.2013.75.

(8) Prabhu, D. D.; Kumar, N. S. S.; Sivadas, A. P.; Varghese, S.; Das, S. Trigonal 1,3,4-Oxadiazole-Based Blue Emitting Liquid Crystals and Gels. *J. Phys. Chem. B* **2012**, *116*, 13071−13080.

(9) Lamarra, M.; Muccioli, L.; Orlandi, S.; Zannoni, C. Temperature Dependence of Charge Mobility in Model Discotic Liquid Crystals. *Phys. Chem. Chem. Phys.* **2012**, *14*, 5368−5375.

(10) Zhang, F. P.; Funahashi, M.; Tamaoki, N. Flexible Field-Effect Transistors From a Liquid Crystalline Semiconductor by Solution Processes. *Org. Electron.* **2010**, *11*, 363−368.

(11) Schmidt-Mende, L.; Fechtenkotter, A.; Mullen, K.; Moons, E.; Friend, R. H.; MacKenzie, J. D. Self-Organized Discotic Liquid Crystals for High-Efficiency Organic Photovoltaics. *Science* **2001**, *293*, 1119−1122.

(12) Kasdorf, O.; Vollbrecht, J.; Ohms, B.; Hilleringmann, U.; Bock, H.; Kitzerow, H. S. Enhanced Organic Light-Emitting Diode Based on a Columnar Liquid Crystal by Integration in a Microresonator. *Int. J. Energy Res.* **2014**, *38*, 452−458.

(13) Sergeyev, S.; Pisula, W.; Geerts, Y. H. Discotic Liquid Crystals: A New Generation of Organic Semiconductors. *Chem. Soc. Rev.* **2007**, *36*, 1902−1929.

(14) Kumar, S. Self-Organization of Disc-Like Molecules: Chemical Aspects. *Chem. Soc. Rev.* **2006**, *35*, 83−109.

(15) Pisula, W.; Tomovic, Z.; Watson, M. D.; Mullen, K.; Kussmann, J.; Ochsenfeld, C.; Metzroth, T.; Gauss, J. Helical Packing of Discotic Hexaphenyl Hexa-Peri-Hexabenzocoronenes: Theory and Experiment. *J. Phys. Chem. B* **2007**, *111*, 7481−7487.

(16) Ruiz, C.; Garcia-Frutos, E. M.; Hennrich, G.; Gomez-Lor, B. Organic Semiconductors Toward Electronic Devices: High Mobility and Easy Processability. *J. Phys. Chem. Lett.* **2012**, *3*, 1428−1436.

(17) Kastler, M.; Pisula, W.; Laquai, F.; Kumar, A.; Davies, R. J.; Baluschev, S.; Garcia-Gutierrez, M. C.; Wasserfallen, D.; Butt, H. J.; Riekel, C.; Wegner, G.; Mullen, K. Organization of Charge-Carrier Pathways for Organic Electronics. *Adv. Mater.* **2006**, *18*, 2255.

(18) van de Craats, A. M.; Warman, J. M.; Fechtenkotter, A.; Brand, J. D.; Harbison, M. A.; Mullen, K. Record Charge Carrier Mobility in a Room-Temperature Discotic Liquid-Crystalline Derivative of Hexabenzocoronene. *Adv. Mater.* **1999**, *11*, 1469−1472.

(19) Warman, J. M.; Piris, J.; Pisula, W.; Kastler, M.; Wasserfallen, D.; Mullen, K. Charge Recombination via Intercolumnar Electron Tunneling through the Lipid-Like Mantle of Discotic Hexa-Alkyl-Hexa-Peri-Hexabenzocoronenes. *J. Am. Chem. Soc.* **2005**, *127*, 14257−14262.

(20) An, Z. Z.; Yu, J. S.; Domercq, B.; Jones, S. C.; Barlow, S.; Kippelen, B.; Marder, S. R. Room-Temperature Discotic Liquid-Crystalline Coronene Diimides Exhibiting High Charge-Carrier Mobility in Air. *J. Mater. Chem.* **2009**, *19*, 6688−6698.

(21) Roy, B.; De, N.; Majumdar, K. C. Advances in Metal-Free Heterocycle-Based Columnar Liquid Crystals. *Chem.—Eur. J.* **2012**, *18*, 14560−14588.

(22) An, Z. S.; Yu, J. S.; Jones, S. C.; Barlow, S.; Yoo, S.; Domercq, B.; Prins, P.; Siebbeles, L. D. A.; Kippelen, B.; Marder, S. R. High Electron Mobility in Room-Temperature Discotic Liquid-Crystalline Perylene Diimides. *Adv. Mater.* **2005**, *17*, 2580.

(23) Kelber, J.; Achard, M. F.; Garreau-de Bonneval, B.; Bock, H. Columnar Benzoperylene-Hexa- and Tetracarboxylic Imides and Esters: Synthesis, Mesophase Stabilisation and Observation of Charge-Transfer Interactions between Electron-Donating Esters and Electron-Accepting Imides. *Chem. - Eur. J.* **2011**, *17*, 8145−8155.

(24) Eccher, J.; Faria, G. C.; Bock, H.; von Seggern, H.; Bechtold, I. H. Order Induced Charge Carrier Mobility Enhancement in Columnar

DOI: 10.1021/acsami.5b03496
ACS Appl. Mater. Interfaces 2015, 7, 16374−16381

Liquid Crystal Diodes. *ACS Appl. Mater. Interfaces* **2013**, *5*, 11935−11943.
(25) Brunet, T.; Thiebaut, O.; Charlet, E.; Bock, H.; Kelber, J.; Grelet, E. Anchoring Transition in Confined Discotic Columnar Liquid Crystal Films. *EPL* **2011**, *93*, 16004.
(26) Cristiano, R.; Eccher, J.; Bechtold, I. H.; Tironi, C. N.; Vieira, A. A.; Molin, F.; Gallardo, H. Luminescent Columnar Liquid Crystals Based on Tristriazolotriazine. *Langmuir* **2012**, *28*, 11590−11598.
(27) Bechtold, I. H.; Eccher, J.; Faria, G. C.; Gallardo, H.; Molin, F.; Gobo, N. R. S.; de Oliveira, K. T.; von Seggern, H. New Columnar Zn-Phthalocyanine Designed for Electronic Applications. *J. Phys. Chem. B* **2012**, *116*, 13554−13560.
(28) Feng, X.; Pisula, W.; Mullen, K. From Helical to Staggered Stacking of Zigzag Nanographenes. *J. Am. Chem. Soc.* **2007**, *129*, 14116.
(29) Li, H. H.; Yan, S. K. Surface-Induced Polymer Crystallization and the Resultant Structures and Morphologies. *Macromolecules* **2011**, *44*, 417−428.
(30) Gbabode, G.; Dumont, N.; Quist, F.; Schweicher, G.; Moser, A.; Viville, P.; Lazzaroni, R.; Geerts, Y. H. Substrate-Induced Crystal Plastic Phase of a Discotic Liquid Crystal. *Adv. Mater.* **2012**, *24*, 658−62.
(31) Grelet, E.; Dardel, S.; Bock, H.; Goldmann, M.; Lacaze, E.; Nallet, F. Morphology of Open Films of Discotic Hexagonal Columnar Liquid Crystals As Probed by Grazing Incidence X-Ray Diffraction. *Eur. Phys. J. E: Soft Matter Biol. Phys.* **2010**, *31*, 343−349.
(32) Cisse, L.; Destruel, P.; Archambeau, S.; Seguy, I.; Jolinat, P.; Bock, H.; Grelet, E. Measurement of the Exciton Diffusion Length in Discotic Columnar Liquid Crystals: Comparison Between Homeotropically Oriented and Non-Oriented Samples. *Chem. Phys. Lett.* **2009**, *476*, 89−91.
(33) Pisula, W.; Zorn, M.; Chang, J. Y.; Mullen, K.; Zentel, R. Liquid Crystalline Ordering and Charge Transport in Semiconducting Materials. *Macromol. Rapid Commun.* **2009**, *30*, 1179−1202.
(34) Koch, N. Organic Electronic Devices and Their Functional Interfaces. *ChemPhysChem* **2007**, *8*, 1438−1455.
(35) Facchetti, A. Semiconductors for Organic Transistors. *Mater. Today* **2007**, *10*, 28−37.

DOI: 10.1021/acsami.5b03496
ACS Appl. Mater. Interfaces 2015, 7, 16374−16381